



## Research article

# A network pharmacology-based approach to explore the molecular mechanism of Aidi injection against prostate cancer

Sheng Guo<sup>a,b,c,1</sup>, Qiuping Zhang<sup>a,b,1</sup>, Xiaolan Li<sup>a,1</sup>, Xiaoxiang Yu<sup>d</sup>, Taijin Lan<sup>e</sup>,  
Wei quan Zhang<sup>a</sup>, Yaoyao Han<sup>a</sup>, Xin Chen<sup>a</sup>, Xin Yang<sup>a,\*\*</sup>, Hongwei Guo<sup>a,\*</sup>

<sup>a</sup> Key Laboratory of Longevity and Aging-related Diseases of Chinese Ministry of Education & Center for Translational Medicine, Guangxi Key Laboratory of Bioactive Molecules Research and Evaluation & College of Pharmacy, Guangxi Medical University, 22 Shuangyong Road, Nanning, 530021, China

<sup>b</sup> The First Affiliated Hospital of Guangxi Medical University, 6 Shuangyong Road, Nanning, 530021, China

<sup>c</sup> Integrated Traditional Chinese and Western Medicine Rehabilitation Department, Jiangbin Hospital of Guangxi Zhuang Autonomous Region, 85 Hedi Road, Nanning, 530021, China

<sup>d</sup> Department of Hematology, 923rd Hospital of the People's Liberation Army, 52 Zhiwu Road, Nanning, 530000, China

<sup>e</sup> School of preclinical medicine, Guangxi University of Chinese Medicine, 179 Mingxiu Dong Road, Nanning, 530001, China

## ARTICLE INFO

## Keywords:

Prostate cancer

Aidi injection

Network pharmacology

JNK and p38 signaling pathway

## ABSTRACT

**Objective:** To explore the molecular mechanism of Aidi injection in the treatment of prostate cancer (PCa).

**Materials and methods:** CCK-8 and colony formation assays were used to detect the effects of Aidi on PC3 and DU145 cells; effects on the cell cycle and apoptosis of DU145 cells were detected by flow cytometry; effects on migration and invasion of PC3 and DU145 cells were detected by wound healing and transwell assay, respectively. The main active components of Aidi, their corresponding targets, and PCa associated pathways were predicted and analyzed by network pharmacology. Then predicted key targets and related signaling pathways were further verified by western blotting. The potential active components of Aidi were predicted by molecular docking technology.

**Results:** Aidi significantly inhibited the proliferation, colony formation, migration, and invasion of PC3 and DU145 cells; Aidi induced apoptosis and cell cycle G2/M phase arrest of DU145 cells. Network pharmacology analysis yielded 36 potential core targets of Aidi against PCa, and the top 10 signaling pathways including MAPK, PI3K-Akt, and HIF-1 $\alpha$  and so on were enriched. Western blotting confirmed that Aidi upregulated the expression levels of p-JNK, p-p38, p-ERK, and ERK in DU145 cells. Molecular docking study showed that kaempferol, (Z)-1-(2,4-dihydroxyphenyl)-3-(4-hydroxyphenyl)prop-2-en-1-one, 7-O-methylisomucronulatol, calycosin, and N-salicylidene-salicylamine can be well binding with JNK and p38.

**Conclusion:** Aidi could inhibit PCa cell proliferation and metastasis through induction of apoptosis and cell cycle arrest, which may be related to activating JNK and p38 signaling pathway.

\* Corresponding author. Guangxi Key Laboratory of Bioactive Molecules Research and Evaluation & College of Pharmacy, Guangxi Medical University, Nanning, 530001, China.

\*\* Corresponding author. Key Laboratory of Longevity and Aging-related Diseases of Chinese Ministry of Education & Center for Translational Medicine, Guangxi Medical University, 22 Shuangyong Road, Nanning, 530021, China.

E-mail addresses: [xiny1301@hotmail.com](mailto:xiny1301@hotmail.com) (X. Yang), [hongweiguog@gxmu.edu.cn](mailto:hongweiguog@gxmu.edu.cn) (H. Guo).

<sup>1</sup> These authors contributed equally to this work.

<https://doi.org/10.1016/j.heliyon.2024.e29720>

Received 20 March 2023; Received in revised form 14 April 2024; Accepted 14 April 2024

Available online 15 April 2024

2405-8440/© 2024 The Authors. Published by Elsevier Ltd. This is an open access article under the CC BY-NC license (<http://creativecommons.org/licenses/by-nc/4.0/>).

## 1. Introduction

Prostate cancer (PCa) is a malignant tumor that occurs in prostatic epithelial tissues and is one of the main malignant tumors in elderly men worldwide. There were about 1,276,000 new cases of PCa worldwide in 2018, and more than 359,000 patients died of PCa [1]. The incidence of PCa in China is less than the global average, but with the aging of the population and changes in diet and lifestyle, it has shown a significant upward trend in recent years, and the outlook is not optimistic [2,3]. The main treatment strategies for PCa are radiotherapy, chemotherapy, androgen deprivation therapy, endocrine therapy, targeted therapy, and immunotherapy [4]. Given the life expectancy of patients and the development of the disease, most patients can only be treated with maximum androgen blockade. In the early stages of androgen deprivation, symptoms can be relieved to some extent; however, after a period of remission (lasting an average of 22.5 months), almost all PCa will eventually develop into castration resistant PCa (CRPC) [5,6]. At present, the main treatment methods for CRPC include enzalutamide, abiraterone, carbataxel, and docetaxel, as well as anti-bone-metastasis therapy and immunotherapy [7]. However, these drugs can only control the tumor for a limited period of time, and the treatment is often accompanied by side effects.

With the continuous development of traditional Chinese medicine (TCM), combinations of TCM and Western medicine have shown advantages in the treatment of cancer, and the importance and status of TCM in the treatment of cancer are gradually increasing. A systematic review of the relevant literature [8] showed that TCM could be used as one of the main treatment methods for CRPC and could improve the quality of life of patients, delay further development of the disease, improve the curative effect, and prolong survival times. Aidi injection, a Chinese patent formulation, is made by purification of effective components of *Mylabris phalerata* Pallas (*Mylabris*), *Panax ginseng* C.A.Mey. (*Ginseng Radix et Rhizoma*), *Eleutherococcus senticosus* (Rupr.&Maxim.) Maxim (*Acanthopanax Senticosi Radix Et Rhizoma Seu Caulis*) and *Astragalus mongholicus* Bunge (*Astragali Radix*). Aidi has been used clinically for the treatment of a variety of tumors, including lung cancer, liver cancer, colorectal cancer, gastric cancer, and ovarian cancer [9]. Although Aidi has been widely used and studied in the clinical treatment of tumors, there has not been any experimental study of its anti-PCa effects at the cellular or animal levels, and there has been a lack of investigation of its molecular mechanism, which currently limits the clinical applications of Aidi in PCa.

As a system biology-based technology, network pharmacology provides an effective method to evaluate the multi-pharmacological effects of TCM at the molecular level [10]. Therefore, in this study, the activity and underlying molecular mechanism of Aidi against PCa were investigated by integrating network pharmacology prediction and molecular biology experimental validations. Molecular docking was employed to validate the binding mode between the active components and their potential targets. These results may provide new insights into the mechanism of action of Aidi in the treatment of PCa.

## 2. Materials and methods

### 2.1. Drugs and reagents

#### 2.1.1. Experimental cell lines and drugs

The human PCa cell lines PC3 and DU145 were provided by the Key Laboratory of Longevity and Age-related Diseases of Chinese Ministry of Education and the Translational Medicine Research Center of Guangxi Medical University. Benign prostatic hyperplasia cells BPH-1 were obtained from Wuhan Sevier Biotechnology Co., Ltd. Aidi injection (batch no. 20190419, and 20230406) was purchased from Guizhou Yibai Pharmaceutical Co., Ltd. Paclitaxel (PTX) injection (Cat No.E161002), were purchased from Jiangsu Aosaikang Pharmaceutical Co., Ltd.(Jiangsu, China).

#### 2.1.2. Main experimental reagents and consumables

Roswell Park Memorial Institute (RPMI)-1640 medium (Cat No. 350-006-CL), penicillin/streptomycin (Cat No. 325-041-EL), were purchased from Beijing Vicente Biotechnology Co., Ltd. (Beijing, China). Fetal bovine serum (FBS) was purchased from Gibco (Grand Island, NY, USA). Annexin V-FITC/PI Apoptosis Detection Kit (Cat No. 550825) and 7-AAD staining solution (Cat No. 340242) were purchased from BD Biosciences (San Jose, CA, USA). Cell Counting Kit-8 (Cat No. C0040) was purchased from Beyotime Biotechnology Co., Ltd. (Shanghai, China). The primary antibodies against the p44/42 MAPK (extracellular-signal-regulated protein kinase [ERK]1/2, Cat. 4695T), p-ERK (Cat. 4370T), C-Jun N-terminal kinase (JNK, Cat. 9252S), p-JNK (Cat. 9255S), p38 (Cat. 9212S), p-p38 (Cat. 4511),  $\beta$ -actin (Cat. 8457), and GAPDH (Cat. 2118L) were purchased from Cell Signaling Technology (Danvers, USA). PD98059 (Cat No.E161002), were purchased from Shanghai Yuanye Biotechnology Co., Ltd.(Shanghai, China).

### 2.2. Experimental method

#### 2.2.1. Study on the chemical composition of Aidi injection

**2.2.1.1. Sample solution.** Take an unopened Aidi, open the bottle and pass it through 0.22  $\mu$ m the test solution is obtained by filtering through a microporous filter.

**2.2.1.2. Test conditions for ultra high performance liquid chromatography quadrupole time-of-flight tandem mass spectrometer (UPLC-Q-TOF/MS).**

### (1) Liquid phase conditions

The chromatographic analysis of the test solution was carried out in the ultra-high performance liquid chromatography analysis system (waters), using the ACQUITY UPLC HSS T3 C18 column (100 mm) as the chromatographic column  $\times$  2.1 mm, 1.8  $\mu$ m i.d., column temperature: 30 °C, mobile phase consisting of aqueous phase (A) containing 0.1 % formic acid and 5 mM ammonium formate, and organic phase of acetonitrile (B), elution conditions: 0–0.3 min: 98 % A; 0.3–7.0 min: 98 %–2 % A; 7.0–9.5 min: 2 %–98 % A; 9.5–10.0 min: 98 % A.

### (2) Mass spectrometry conditions

The mass spectrometric analysis of the test solution was carried out in the XEVO G2-S QTOF mass spectrometer (Waters Corp, Manchester, United Kingdom) equipped with an electric spray ion source (ESI). The mass spectrometry detection parameters are set to: collision voltage, 3.0 kV; Sample and extraction voltage, 30 and 4.0 V. Desolvent gas rate and temperature, 600 L/h and 350 °C; Source temperature, 100 °C; Scanning time, 0.15 s; Scanning delay, 0.02 s, we used leucine enkephalin as a locking block ( $m/z$  556.2771 in cationic mode and  $m/z$  554.2615 in anionic mode), with a concentration of 0.5 mg/mL and a flow rate of 10  $\mu$ L/min. Using the MSE collection mode for mass spectrometry data detection, the primary mass spectrometry data collection range is  $m/z$  100–1200, while the secondary mass spectrometry data collection range is  $m/z$  10–1200.

**2.2.1.3. Analysis and Identification of Aidi's main chemical components.** Wash the test solution according to the conditions of ultra-high performance liquid chromatography time-of-flight mass spectrometry to obtain primary and secondary mass spectrometry data. Analyze the chemical composition by comparing the measured mass to charge ratio with the chemical composition mass spectrometry information collected in databases and literature.

#### 2.2.2. Cell proliferation assay

The CCK-8 method was used to detect the proliferation of PC3, DU145, and BPH-1 cells treated with different drugs. We adjusted the concentration of PC3, DU145, and BPH-1 cells to  $3 \times 10^4$ /mL, cell suspension at 100  $\mu$ L/well was inoculated into 96-well plates and incubated overnight. Then, cells were treated with different concentrations (Aidi: 0, 25, 50, 75, 100, 150, 200, and 300  $\mu$ L/mL; PTX: 0, 2.5, 5, 10, 20, 40, 60, 80, 120, and 160 ng/mL) of drugs, and culture was continued for 24 h, 48 h, and 72 h. Besides, Aidi combined with ERK inhibitor PD98059 experiment, PC3 and DU145 cells were pretreated with ERK inhibitor PD98059 (40  $\mu$ M) for 1 h, and then cotreated with Aidi for 48 h. Then, 10 % CCK-8 medium was added to the culture medium, followed by incubation at 37 °C for 1 h. The optical density (OD) at 450 nm was measured with a microplate reader, and the relative activity of the cells was calculated using the following formula:

$$\text{Relative cell activity (\%)} = \frac{\text{OD value of administration group} - \text{OD value of blank control group}}{\text{OD value of solvent control group} - \text{OD value of blank control group}} \times 100\%$$

GraphPad Prism 8 was used to plot relative activity curves for cells, and SPSS 25 was used to calculate the half-maximal inhibitory concentration (IC<sub>50</sub>) of Aidi against PCa and BPH-1 cells.

#### 2.2.3. Colony formation assay

The effect of Aidi on the clonogenic ability of PC3 and DU145 cells was detected by plate clonogenic assay. As previously mentioned [11], PC3 and DU145 cells were inoculated into 6-well plates at a density of 150 cells/well. After 24 h of culture, 2 mL RPMI-1640 complete medium containing different concentrations of Aidi (20 and 40  $\mu$ L/mL) were added to each well. A negative control group without Aidi was also set up. All groups of cells were cultured in a 37 °C, 5 % CO<sub>2</sub> incubator. The culture was terminated when multiple clonal clumps were observed in the microplates, followed by staining with 0.05 % crystal violet for 30 min. Image J software was used to calculate the number of cell clones, GraphPad Prism 8 was used to draw a statistical chart of the cloning rates, and SPSS 25 was used to analyze the experimental results.

#### 2.2.4. Cell cycle and apoptosis analysis

Flow cytometry (FACScan; BD Biosciences) was used to detect the effect of Aidi on DU145 cell cycle and apoptosis. As previously described [12], DU145 cells were inoculated into a 6-cm cell culture dish at a cell concentration of  $1.5 \times 10^5$ /mL. After 16 h of culture, 3.5 mL medicated culture medium was added to the cells in the experimental group, and the control group received the same amount of culture medium, for 48 h. Then cell cycle distribution was measured using 7-AAD staining, and the proportion of apoptotic cells was determined using an Annexin V-FITC/7-AAD apoptosis detection kit according to the manufacturer's protocol. The raw flow cytometry data were analyzed using Flow Jo software, and the cell proportions in each phase were analyzed with GraphPad Prism 8.

#### 2.2.5. Cell migration assay

Cell migration was assessed by wound-healing assay as previously mentioned [13]. Briefly, PC3 and DU145 cells were seeded in 6-well plates according to the cell density of  $6 \times 10^5$  cells/well and  $8 \times 10^5$  cells/well, respectively. The 6-well plates were cultured at 37 °C for 24 h in 5 % CO<sub>2</sub> incubator. Then 20  $\mu$ g/mL of mitomycin was added to the 6-well plates and incubated at 37 °C for 2 h. Then a vertical wound was created using a sterile 10  $\mu$ L pipette tip. Cells were treated with serum-free RPMI-1640 medium containing 35 or

70  $\mu\text{L}/\text{mL}$  of Aidi for PC3 cells, and 25  $\mu\text{L}/\text{mL}$  or 50  $\mu\text{L}/\text{mL}$  of Aidi for DU145 cells, and the control group of serum-free medium was set. Cells were photographed using a microscope at three time points (0, 12, and 24 h). The area of migration was measured and analyzed with Image J software.

### 2.2.6. Cell invasion assay

Invasion assay was determined using transwell chambers coated with Matrigel as described previously [14]. Briefly, after 24, 48, and 72 h pre-treatment with different concentrations of Aidi (65 or 130  $\mu\text{L}/\text{mL}$  for PC3 cells and 40 or 80  $\mu\text{L}/\text{mL}$  for DU145 cells), tumor cells were collected and re-suspended in serum free cell culture media. A total of  $8 \times 10^4$  cells in 100  $\mu\text{L}$  were added in the upper chamber, and 600  $\mu\text{L}$  of medium containing 10 % FBS was added in the lower chamber. The cells were allowed to invade for 24 h, then invaded cells were stained with 0.1 % crystal violet and counted in five random microscopic fields.

### 2.2.7. Network pharmacology prediction

We used TCM Systems Pharmacology (TCMSP) Database (<http://old.tcmssp-e.com/tcmssp.php>, accessed on February 11, 2020) and TCM Integrated Database (TCMID) (<http://119.3.41.228:8000/tcmid/>, accessed on February 13, 2020) to collect the active ingredients of Aidi. Target compounds were screened using the criterion of oral bioavailability  $\geq 30\%$ . Target proteins corresponding to the active ingredients were queried through the TCMSP database. The UniProt database (<http://www.uniprot.org/>, accessed on February 14, 2020) was used to query the gene name corresponding to the target protein. We then searched the GeneCards database (<http://www.genecards.org/>, accessed on February 11, 2020) and Online Mendelian Inheritance in Man (OMIM) database (<https://www.omim.org/>, accessed on February 12, 2020) using the keyword “prostatic cancer” to screen gene targets related to PCa. Furthermore, the overlapped targets both related to the candidate compounds and PCa were kept for network construction and analysis. The protein-protein interaction (PPI) network was constructed by Search Tool for the Retrieval of Interacting Genes/Proteins database (STRING, <https://string-db.org/>, Version 11.0) with medium confidence 0.400 by default. All the networks were created and visualized via Cytoscape (<https://cytoscape.org/>, Version 3.2.1) a general platform for complex network analysis and visualization [15]. The Kyoto Encyclopedia of Genes and Genomes (KEGG) pathway enrichment analysis of intersection genes was carried out.

### 2.2.8. Western blot analysis

Western blot was used to verify the predicted key targets and related signaling pathways. As previously described [16], after treatment with Aidi for 48 h, DU145 cells were collected and the total cell proteins were extracted and quantified by bicinchoninic acid (BCA) method. Protein samples were separated with SDS-PAGE and transferred to polyvinylidene fluoride membranes. Phosphorylated proteins were blocked with 5 % BSA solution, and other proteins were blocked with 5 % skimmed milk for 1 h. Proteins were incubated with primary antibody diluent (dilution ratio 1:1000) for about 12 h, then incubated in secondary antibody diluent (dilution ratio 1:5000) for 1 h, followed by chemiluminescence. Image J software was used to analyze the gray values of the target bands and the internal reference protein. GraphPad Prism 8 was used to plot statistics. The experimental results were statistically analyzed with SPSS 25.

### 2.2.9. Molecular docking

The compound structure (mol2 format) was obtained in the TCMSP database (accessed on April 22, 2021). The protein crystal structure (in pdb format) was extracted from Protein Data Bank (PDB) database (<https://www.rcsb.org/>, accessed on April 22, 2021). The compound structure and crystal structure were imported into Sybyl X2.0 software for molecular docking. The total score value of Surflex Dock molecular docking module is greater than 6.0 to evaluate the ability of ligands and receptors to bind, screen the possible

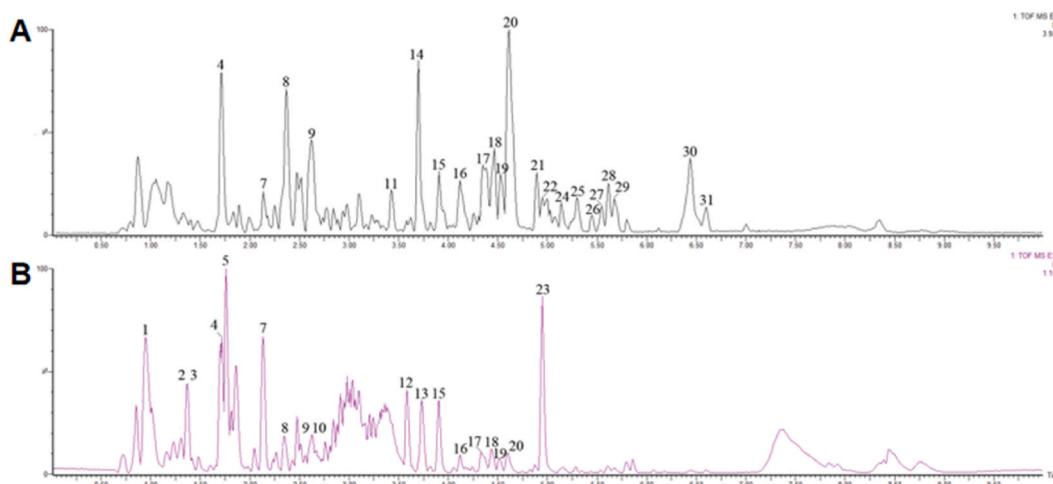
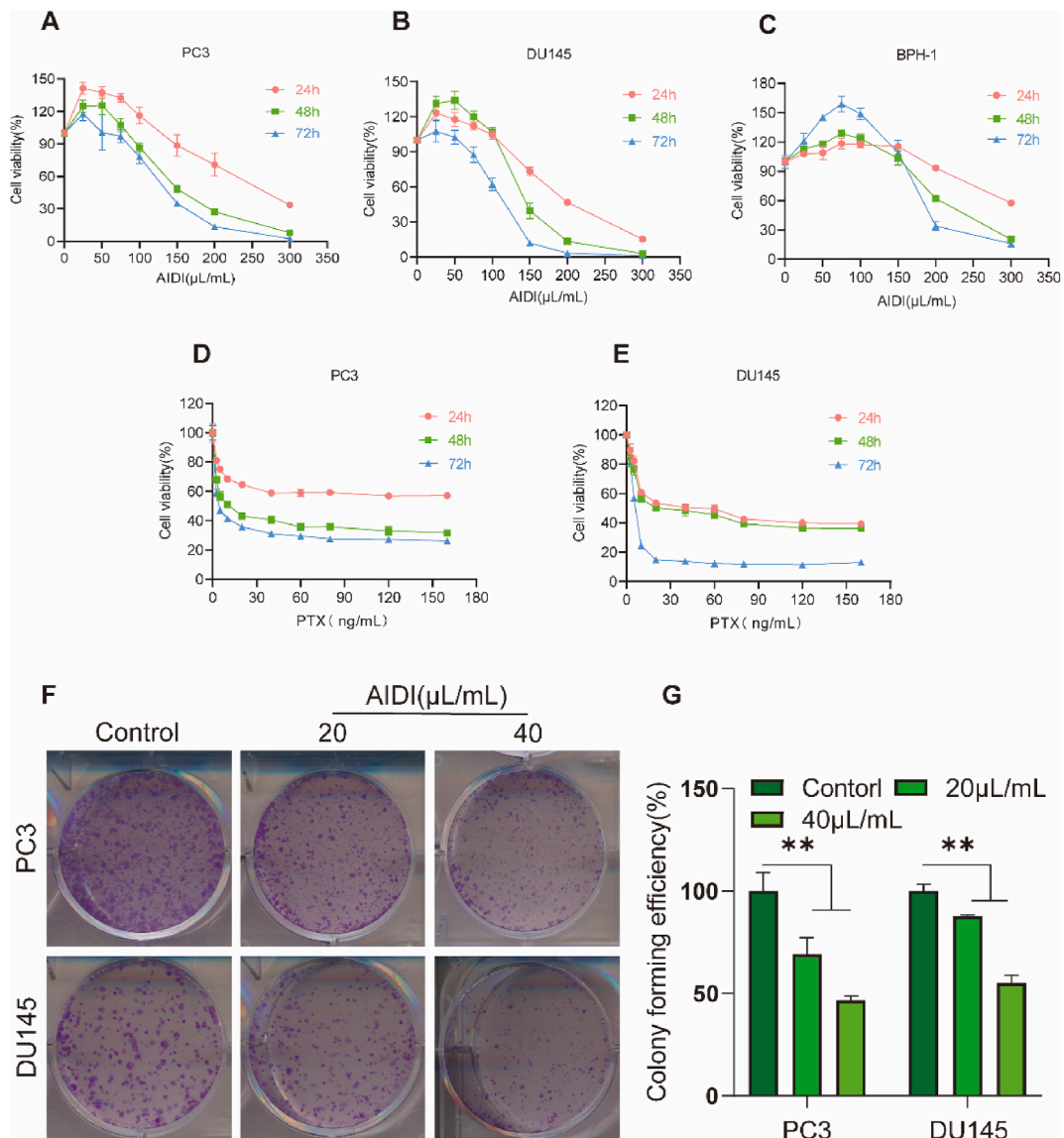


Fig. 1. BPI chromatogram of Aidi injection chemical composition. (A: negative ion mode, B: positive ion mode).

effective components of Aidi's anti prostate cancer, and visualize the docking mode with Pymol software.

### 2.3. Statistical method

Statistical analysis was performed using SPSS 25. Data were presented as mean  $\pm$  standard deviation (SD). The two-tailed unpaired Student's *t*-test was used for comparisons between two groups, the one-way ANOVA was used for comparisons between multiple groups, and the difference was statistically significant at  $P < 0.05$ .



**Fig. 2.** Aidi inhibited the viability of PCa and BPH-1 cells. (A, B, and C): PC3, DU145 and BPH-1 cells were treated with different concentrations of Aidi (0–300  $\mu\text{L/mL}$ ) for 24, 48 and 72 h, and cell viability was detected using the CCK-8 assay. (D and E) PC3 and DU145 cells were treated with different concentrations of PTX (0–160 ng/mL) for 24, 48 and 72 h, and cell viability was detected using the CCK-8 assay. (F) The effects of Aidi on the clonogenic ability of PC3 and DU145 cells were detected by plate cloning assay. (G) The statistical chart of the colony formation rate of PC3 and DU145 cells.  $**P < 0.01$  compared with control group.

### 3. Results

#### 3.1. UPLC-Q-TOF/MS analysis results

##### 3.1.1. Aidi chemical composition analysis chromatogram

After using the UPLC-Q-TOF/MS analyzer to detect Aidi, representative peak intensity chromatograms (BPI) of the collected information in positive and negative ion modes were obtained, as shown in Fig. 1A and B.

##### 3.1.2. Aidi chemical composition

Under positive and negative ion modes, 19 and 23 chemical components of Aidi were identified, including Ginsenoside Rf, Ginsenoside C, Ginsenoside Rh1, Ginsenoside F1, 9,10,13-TriHOME, Pyroglutamic acid, Guanosine, Phenylalanine, Chlorogenic acid, Cryptochlorogenic acid, Astrapterocarpan, etc. 31 compounds were obtained by removing duplicate components (one of which has an unknown compound name). Detailed information on each chemical component is shown in Supplemental Table 1, Supplemental Table 2.

#### 3.2. Aidi inhibited the viability of PCa cells

CCK-8 assay was utilized to evaluate the antiproliferative effect of Aidi on PC3 and DU145 cells. As shown in Fig. 2A and B, Aidi injection significantly reduced the cell viability of PC3 and DU145 cells in time- and dose-dependent manners. To further verify the effect of Aidi on non-cancerous cells, the proliferation of prostate hyperplasia cells BPH-1 treated with Aidi was detected by CCK-8 assay. As shown in Fig. 2C and Table 1, the IC<sub>50</sub> values of BPH-1 cells were much greater than those of PC3 and DU145 cells. Besides, The effect of the IC<sub>50</sub> values obtained by PC3 and DU145 cells (Refer to Table 1) on the proliferation of BPH-1 was detected by CCK8 assay. The results showed that the determined IC<sub>50</sub> values of 24 h have a little death effect on non-cancerous cells. Contrary to the above results, the IC<sub>50</sub> values at 48 and 72 h promoted the proliferation in BPH-1 cells, suggesting that it not only inhibited PCa cells but also had a beneficial effect on BPH-1 cells (Supplemental Fig. 1).

In addition, the effect of PTX on the proliferation of PC3 and DU145 cells was detected by CCK-8 assay. As shown in Fig. 2D and E, the viability of PC3 and DU145 cells was significantly inhibited by PTX and showed in both dose- and time-dependent manners. After 72 h of PTX treatment, the IC<sub>50</sub> values of PC3 and DU145 cells were  $4.38 \pm 0.47$  ng/mL and  $5.97 \pm 0.20$  ng/mL, respectively (Table 2).

In order to further evaluate the effect of Aidi on population dependence and proliferation ability in PCa cells, plate cloning experiments were performed. The results are shown in Fig. 2F and G. After treatment with Aidi, the clonogenic ability of PC3 and DU145 cells decreased significantly, and the number and size of clones were less than those of the control group ( $P < 0.01$ ). The clone formation rates of PC3 and DU145 cells treated with 40  $\mu$ L/mL of Aidi were 46.66 % and 55.19 %, respectively.

#### 3.3. Aidi induced the apoptosis and cell cycle arrest in DU145 cells

To investigate the underlying mechanism by which Aidi inhibited the PCa cell proliferation and cloning formation, we first assessed the effect of Aidi on cell cycle using the flow cytometry and the results were shown in Fig. 3A and B. After treatment with Aidi at a concentration of 40  $\mu$ L/mL or 80  $\mu$ L/mL for 48 h, the proportion of DU145 cells in G0/G1 phase decreased and the proportion in G2/M phase increased significantly compared with the control group. These results suggested that Aidi could induce G2/M phase arrest in DU145 cells.

Furthermore, flow cytometry was used to verify the influence of Aidi on the apoptosis of DU145 cells, and the results were shown in Fig. 3C and D. After treatment for 48 h with 80  $\mu$ L/mL of Aidi, the apoptosis rate of DU145 cells was significantly greater than that of the control group, as demonstrated by the fact that the proportion of early apoptotic cells in the lower right quadrant showed a statistically significant increase ( $P < 0.01$ ). These results suggested that Aidi could induce the apoptosis of DU145 cells.

#### 3.4. Aidi inhibits the migration of PCa cells

In order to explore the effects of Aidi on the metastasis of PCa cells, we first observed its effects on the migrative ability of PC3 and DU145 cells by wound healing assay. As shown in Fig. 4, Aidi inhibited the migration of PC3 and DU145 cells to varying degrees: after treatment with Aidi for 12 h and 24 h, the migration rate of PC3 cells was less than that of the control group (Fig. 4A, B,  $P < 0.01$ ). DU145 cells were treated for 24 h with various concentrations of Aidi. The migration rate of the cells treated with 50  $\mu$ L/mL of Aidi was significantly less than that of the control group (Fig. 4C, D,  $P < 0.01$ ).

**Table 1**

The IC<sub>50</sub> values of Aidi on PCa and BPH-1 cells ( $\mu$ L/mL).

Cell lines	24 h	48 h	72 h
PC3	251.32 $\pm$ 12.47	154.24 $\pm$ 3.33	132.71 $\pm$ 3.87
DU145	193.65 $\pm$ 4.39	135.12 $\pm$ 9.8	107.22 $\pm$ 4.41
BPH-1	363.95 $\pm$ 5.37	231.73 $\pm$ 5.96	207.28 $\pm$ 5.74

**Table 2**  
The IC<sub>50</sub> values of PTX on PCa cells (ng/mL).

Cell lines	24 h	48 h	72 h
PC3	292.27 ± 65.61	13.40 ± 1.46	4.38 ± 0.47
DU145	48.95 ± 0.94	35.85 ± 4.43	5.97 ± 0.20

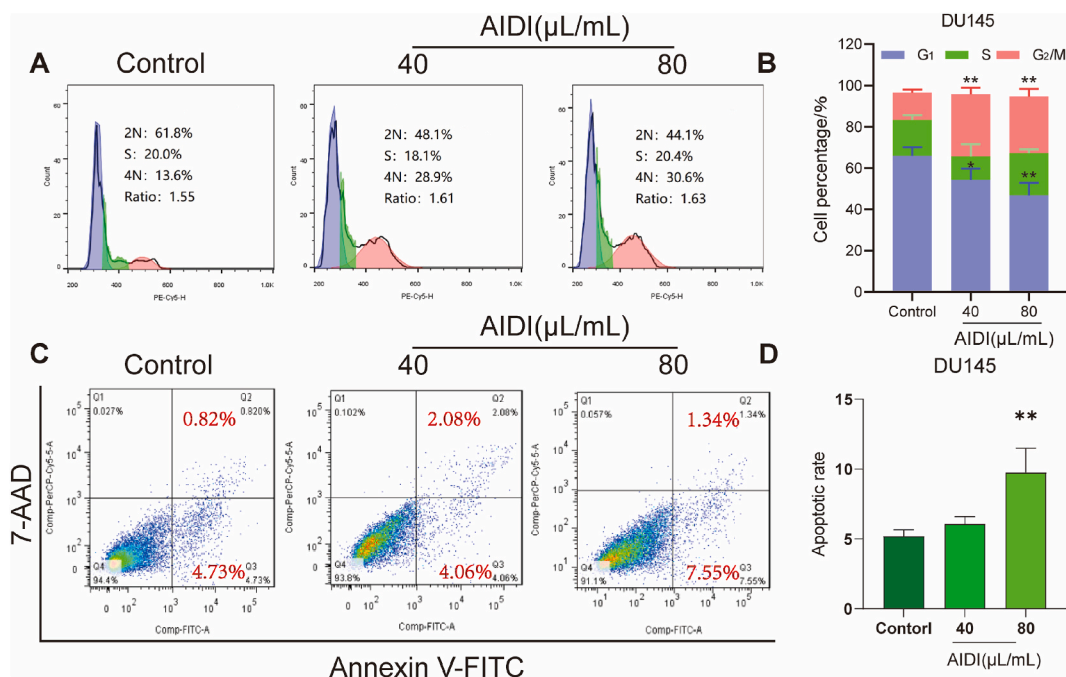


**Fig. 3.** Aidi induced the apoptosis and cell cycle arrest in DU145 cells. (A) DU145 cell cycle of flow chart treated by Aidi injection for 48h. (B) The statistical chart of DU145 cell cycle distribution. (C) Flow chart of DU145 cell apoptosis after treatment with Aidi for 48 h. (D) Statistical chart of DU145 cell apoptosis rate. \*\* $P < 0.01$  compared with control group.

### 3.5. Aidi inhibited the invasion of PCa cells

Transwell assay was used to detect the effects of Aidi on the invasive ability of PC3 and DU145 cells. As shown in Fig. 5, Aidi inhibited the invasion of PC3 and DU145 cells to varying degrees: after Aidi treatment for 24 h, 48 h, and 72 h, the invasion rate of PC3 cells was significantly less than that of the control group (Fig. 5A, B,  $P < 0.01$ ). With the exception of the group treated with Aidi at a low-concentration (40 μL/mL) for 48 h, the invasion rate of DU145 cells in all groups was less than that of the control group, and the difference was statistically significant (Fig. 5C, D,  $P < 0.01$ ).

### 3.6. Network pharmacology analysis results

#### 3.6.1. Active ingredients and targets screening

To further explore the molecular mechanism underlying the inhibition of proliferation and metastasis by Aidi, we used network pharmacology to predict the possible targets and signaling pathways. A total of 128 ingredients of Aidi were collected according to the ADME threshold of  $OB \geq 30\%$ , which were shown in Supplemental Tables 3 and a herb-ingredient network diagram was shown in Fig. 6A. A total of 430 corresponding targets were predicted to be hit by the 128 ingredients in Aidi, and the detailed information about the targets was shown in Supplemental Table 4. The ingredient-target network was shown in Fig. 6B.

We also searched the GeneCards and OMIM databases using the key word "prostatic cancer" to find 1954 genes related to PCa. A network diagram of PCa and its corresponding targets was shown in Fig. 6C. The Venn analysis of Aidi's 430 target genes and the 1954 PCa-related genes was illustrated in Fig. 6D; 148 shared genes were obtained. These 148 genes were analyzed using the STRING database to identify protein interactions, and a PPI network diagram was constructed using Cytoscape (Fig. 6E), including 131 nodes and 2897 connections. According to the average degree of freedom of 1.5, a total of 36 core targets were obtained and shown in Supplemental Table 5. These core targets corresponded to a total of 128 chemical components in Aidi.

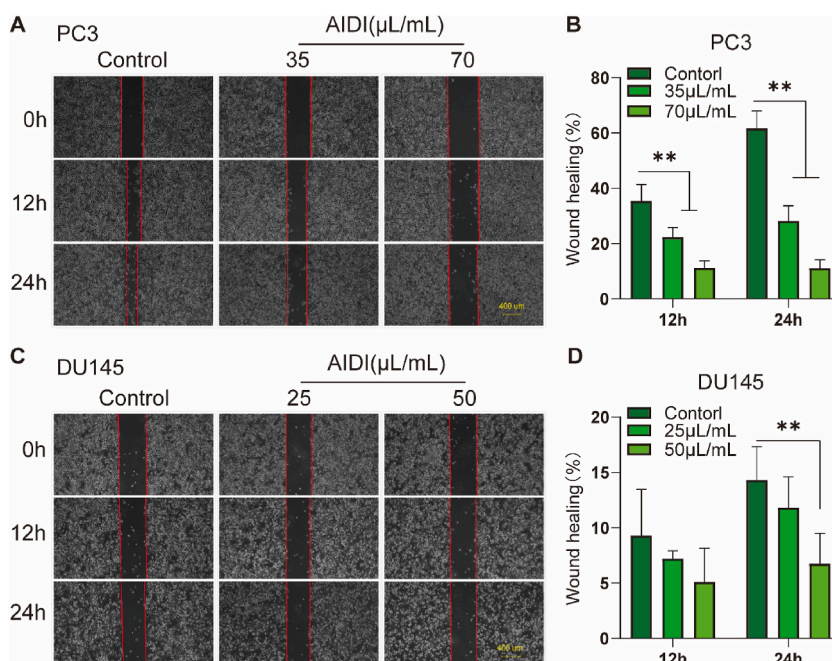


**Fig. 4.** Effects of Aidi injection on migration ability of PCa cells. (A, B) Effects of Aidi on the migration ability of PC3 cells and statistical chart of wound healing. (C, D) Effects of Aidi on the migration ability of DU145 cells and statistical chart of wound healing.  $**P < 0.01$  compared with control group.

### 3.6.2. Pathway enrichment analysis results

The above 36 core targets were subjected to KEGG enrichment analysis, and a total of 158 signaling pathways were obtained. The top 10 enriched signaling pathways were shown in Fig. 6F, among which MAPK and PI3K-Akt signaling pathways are closely related to tumor proliferation, cell cycle, apoptosis, and metastasis.

### 3.7. Aidi upregulated MAPK signaling pathway in DU145 cells

Subsequently, we used Western Blot to verify the expression of key proteins and their phosphorylation in MAPK signaling pathway. The results showed that Aidi upregulated the protein expression of *p*-JNK, *p*-p38, ERK, and *p*-ERK in DU145 cells (Fig. 7A and B,  $P < 0.01$  or  $0.05$ ), suggesting that Aidi may induce PCa apoptosis and cycle arrest by regulating the MAPK signaling pathway, thereby inhibiting the growth and metastasis of PCa.

### 3.8. Molecular docking results

Western Blot experiments confirmed that Aidi regulates the expression and activities of ERK, JNK, and p38 in DU145 cells. The active ingredients of key proteins ERK (MAPK1), JNK (MAPK8), and p38 (MAPK14) as predicted by network pharmacology are shown in Supplemental Table 6. The nine compounds listed, namely quercetin, 3-phenyl-4-azafluorene, isorhamnetin, 7-O-methyl-isomucronulatol, formononetin, calycosin, (Z)-1-(2,4-dihydroxyphenyl)-3-(4-hydroxyphenyl)prop-2-en-1-one, N-salicylidene-salicylamine, and kaempferol, are potential active components of Aidi that could inhibit PCa (Fig. 8A). In order to further study the relationship between each target (ERK, JNK, and p38) and the nine components, we used Sybyl X2.0 software for molecular docking. The crystal structures obtained from the PDB database were ERK (PDB ID: 1TVO), JNK (PDB ID: 3PZE), and p38 (PDB ID: 1WBW). The detailed docking scores for pairs of receptors and ligands are shown in Supplemental Table 7. JNK showed good binding to kaempferol (Fig. 8B), and p-38 showed good binding to (Z)-1-(2,4-dihydroxyphenyl)-3-(4-hydroxyphenyl)prop-2-en-1-one, 7-O-methyl-isomucronulatol, calycosin, and N-salicylidene-salicylamine (Fig. 8C-F).

## 4. Discussion

PCa is among the major malignant tumors that endanger men's health. At present, drugs used in the clinical treatment of PCa include androgen-blocking drugs, chemotherapy drugs, targeted inhibitory drugs, and immunotherapy drugs. Although they have improved the survival rates of PCa patients to varying degrees, these drugs often cause adverse reactions, resulting in a serious decline in the quality of life of patients. TCM has obvious advantages in improving the quality of life of patients and reducing the occurrence of side effect. Aidi has been widely used in the treatment of lung cancer, liver cancer, gastric cancer, colon cancer, B-cell lymphoma,



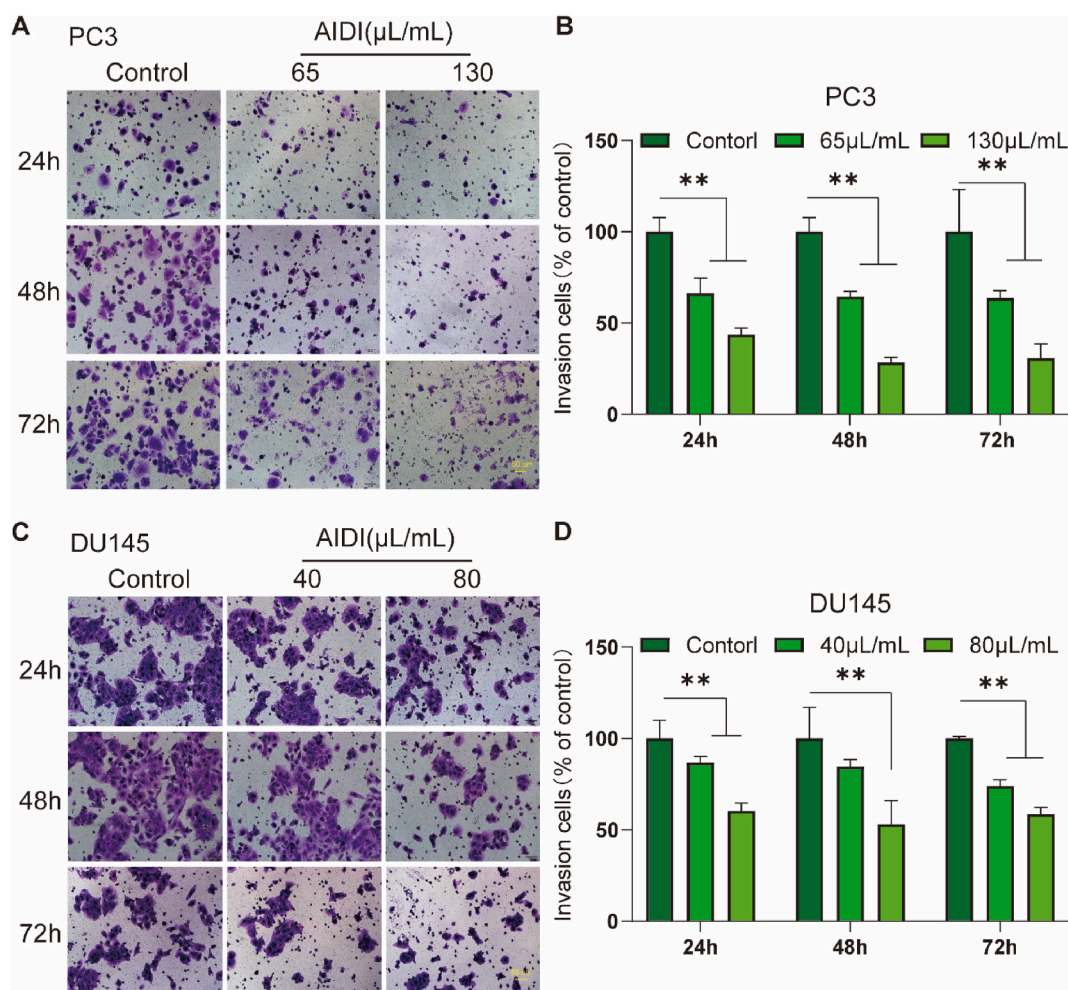


**Fig. 5.** Effects of Aidi injection on the invasion of PCa cells. (A, B) Effects of Aidi treatment at different concentrations on PC3 cell invasion and statistical chart showing results of transwell assay. (C, D) Effects of Aidi treatment at different concentrations on DU145 cell invasion and statistical chart showing results of transwell assay.  $**P < 0.01$  compared with control group.

breast cancer, ovarian cancer, and other tumors; however, there have been few clinical reports and mechanism studies on its function in PCa. Therefore, this study used a network pharmacology method combined with modern molecular biology technology to explore the active ingredients and molecular mechanism of Aidi's inhibition of PCa, in order to provide a reference for clinical treatment of PCa with Aidi.

The occurrence and development of tumors are due to the rapid proliferation of cells after mutation, their invasion beyond the boundaries of normal tissues to surrounding organs and tissues, and even migration and spread to the whole body [17–20]. In addition, inhibition of apoptotic cell death mechanisms and changes in apoptotic state are among the characteristics of tumor occurrence and development and are related to tumor therapy resistance. Therefore, controlling the biological behavior of tumor cells is an effective approach to treatment. The results of the CCK-8 experiment in this study showed that Aidi treatment significantly inhibited the proliferation of PC3 and DU145 cells, with a time- and dose-dependent manner. Plate clone formation assay showed that Aidi could significantly inhibit the clone formation ability of PC3 and DU145 cells. We further used flow cytometry to detect whether Aidi inhibited the proliferation of PCa cells by inducing apoptosis and cycle arrest. The results showed that Aidi could arrest the DU145 cells in G2/M phase and also induced DU145 cells of apoptosis. We also found that Aidi could inhibit the migration and invasion of PC3 and DU145 cells to varying degrees.

We used a network pharmacology approach to further explore the potential molecular mechanism of Aidi in the treatment of PCa. Based on systems biology, network pharmacology selects key genes and related signaling pathways of drugs and diseases from the relevant biological databases. The principles of network pharmacology are consistent with the systematicness and integrity of TCM, and it is a reliable method and a powerful tool for research on TCM. In the present study, potential targets of Aidi against PCa were screened based on network pharmacology, and the most of predicted targets (including the MAPKs, AKT1, MYC, CASP3, EGFR, MMP2/9, and CCL2) were related to tumor cell proliferation, the cell cycle, apoptosis, and metastasis [21–23]. Subsequently, we performed

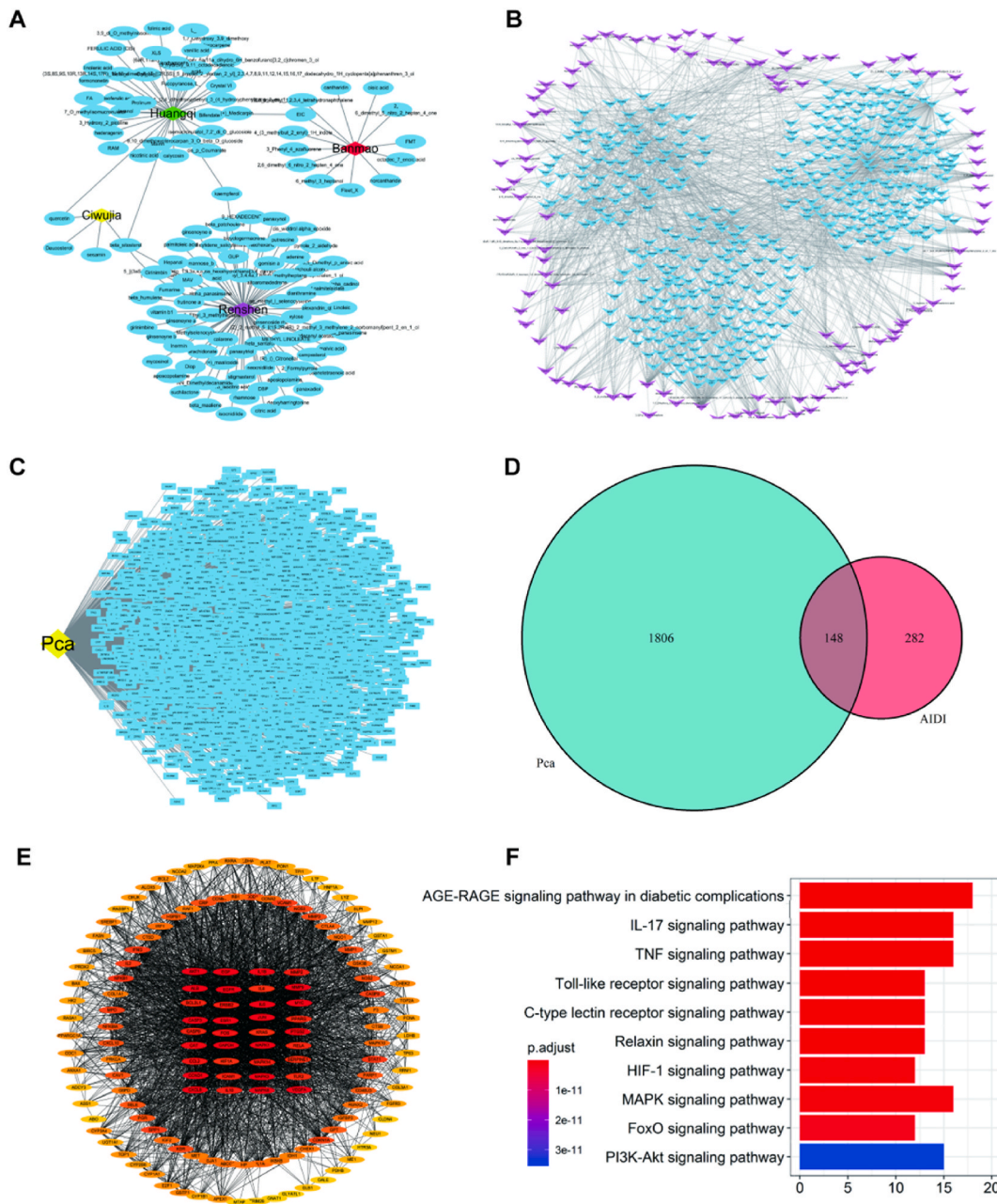


**Fig. 6.** Network pharmacology prediction results. A: Herb-ingredient network diagram (diamond nodes indicate herbs in Aidi: red, cantharidin; purple, ginseng; green, Astragalus; yellow, Acanthopanax senticosus) and blue circles indicate the corresponding ingredients. B: Ingredient-target network diagram (purple nodes represent components and blue node represents the corresponding targets). C: Target network diagram for PCa (the yellow node represents PCa and blue nodes represent targets in PCa). D: Venn diagram of target genes and PCa-related genes. E: The network diagram of protein-protein interaction within the common target (the color of nodes in the diagram changes from red to yellow according to the degree of freedom, and the middle node is the selected 36 key common targets). F: Signaling pathways identified by KEGG enrichment analysis (Note: The longer the length of the histogram, the more the number of key genes enriched; The redder the histogram, the smaller the adjusted p-value. (For interpretation of the references to color in this figure legend, the reader is referred to the Web version of this article.)

KEGG pathway enrichment analysis on these 26 core targets to further explore the related signaling pathways involved in the inhibition of PCa by Aidi. A total of 158 signaling pathways were predicted, the top 10 signaling pathways including MAPK and PI3K-Akt signaling pathway are closely related to the occurrence and development of tumors [24,25]. MAPKs are a class of serine/threonine protein kinases including p38 kinase (p38MAPK), ERK, and JNK that have key roles in the corresponding signaling pathways. The ERK signaling pathway regulates cell proliferation and differentiation, and the p38MAPK and c-Jun N-terminal kinase signaling pathways

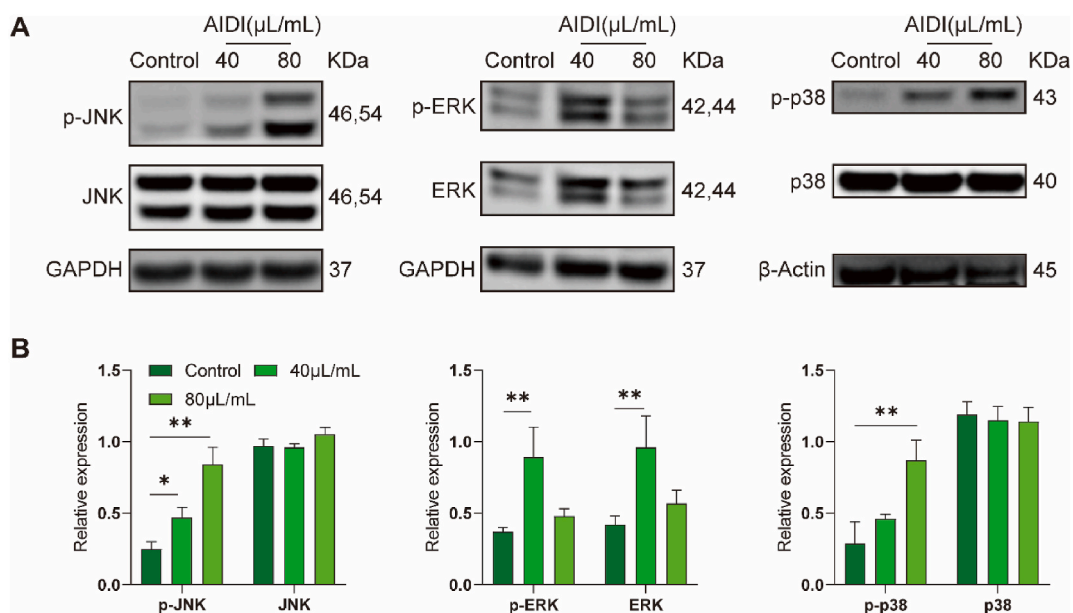


**Fig. 7.** Aidi upregulated MAPK signaling pathway *in vitro*. DU145 cells were treated with Aidi for 48 h, the expressions and activities of JNK, ERK and p38 in MAPK signaling pathway were detected by Western Blot. GAPDH and  $\beta$ -actin were used as controls. A: Representative Western Blot bands for MAPK signaling pathway; B: Bar plot of Western Blot results. \* $P < 0.05$ , \*\* $P < 0.01$  compared with control group.

regulates extracellular environment stimuli. Recent research has shown that the MAPK signaling pathway has a bidirectional regulatory role in the occurrence and progression of the disease. Studies have also shown that the activation of the MAPK signaling pathway promotes disease progression. For example, stimulation of lipopolysaccharide can lead to phosphorylation of ERK, JNK, and p38 proteins, increase the expression of inflammation-related genes, and promote the secretion and expression of inducible cytokines and inflammatory mediators [26]. In-depth study of MAPK has shown that the activation of MAPK signaling pathway can also inhibit the development of disease. The results of the present study showed that Aidi treatment inhibited proliferation, migration, and invasion of PCa cells and increased apoptosis; it also increased p-p38, p-JNK, p-ERK, and ERK protein levels, which suggested that Aidi could inhibit PCa cells by inducing activation of the MAPK signaling pathway. ERK activation is reported to contribute to the proliferative and antiapoptotic activity of tumor cells in many studies [27]. However, in our study, Aidi increased p-ERK and ERK protein levels and achieved opposite experimental results. Therefore, we have determined the effect of PD98059 which is ERK inhibitor on the Aidi-induced cell proliferation by CCK8 assay. The results showed that Aidi significantly inhibited the proliferation of DU145 and PC3 cells, while PD98059 could not reverse this effect (Supplemental Fig. 2). Therefore, we speculate that Aidi does not inhibit the proliferation of PCa cells through the ERK signaling pathway.

Alterations in the MAPK signaling pathway are a striking feature of many cancer cells, including PCa cells [28–30]. Research has found that curcumin induces apoptosis of human hepatoma Huh7 cells by activating p38 MAPK signaling pathway [31]. Ghatan et al. [32] showed that p38 induces apoptosis by promoting the translocation of Bax to mitochondria and causing the activation of caspase family proteins. *In vitro* assays demonstrated that JNK overexpression promoted cell viability and invasion as well as the protein expressions of extracellular signal-regulated kinase (ERK) and matrix metalloproteinase 1 (MMP1) in PC-3 cell lines [33]. Thus, we hypothesized that Aidi could inhibit the proliferation of PCa cells by activating the p38 and JNK signaling pathway and regulating key proteins related to this pathway.

In order to further study the relationship between each target (JNK and p38) and the nine components identified in the present study, we carried out molecular docking. The results showed that JNK bound well to kaempferol, whereas p38 bound well to (Z)-1-(2,4-dihydroxyphenyl)-3-(4-hydroxyphenyl)prop-2-en-1-one, 7-O-methylisomucronulatol, calycosin, N-salicylidene-salicylamine. Therefore, these five components may be potential pharmacodynamic substances of Aidi that may account for its activity against PCa. (Z)-1-(2,4-dihydroxyphenyl)-3-(4-hydroxyphenyl)prop-2-en-1-one is a unique active ingredient of Astragalus. There have been few relevant reports on this component to date; however, its molecular docking results in the present study generally showed higher scores than other components, suggesting that it may be the active ingredient in the activity of Aidi against PCa. In the drug-ingredient-target-disease network, 7-O-methylisomucronulatol was associated with target genes including PPARG and androgen receptor (AR). Positive AR expression may be associated with lymph node metastasis and lung cancer progression [34]. PCa is an androgen-dependent disease; thus, as androgen acts through AR [35], it is reasonable to speculate that 7-O-methylisomucronulatol may have an anti-PCa effect. This requires further experimental research. Kaempferol exerts its anti-cancer role mainly by regulating the transcription of cyclooxygenase-2, inhibiting the function and expression of P-glycoprotein, inhibiting interleukin-4 anti-cell proliferation, inducing apoptosis, intervening in cell signal transduction, enhancing the activity of tumor suppressor genes, and inhibiting the expression of oncogenes. It inhibits tumor cell proliferation by inducing apoptosis, as validated in studies of tumor cells [36]. Calycosin is an

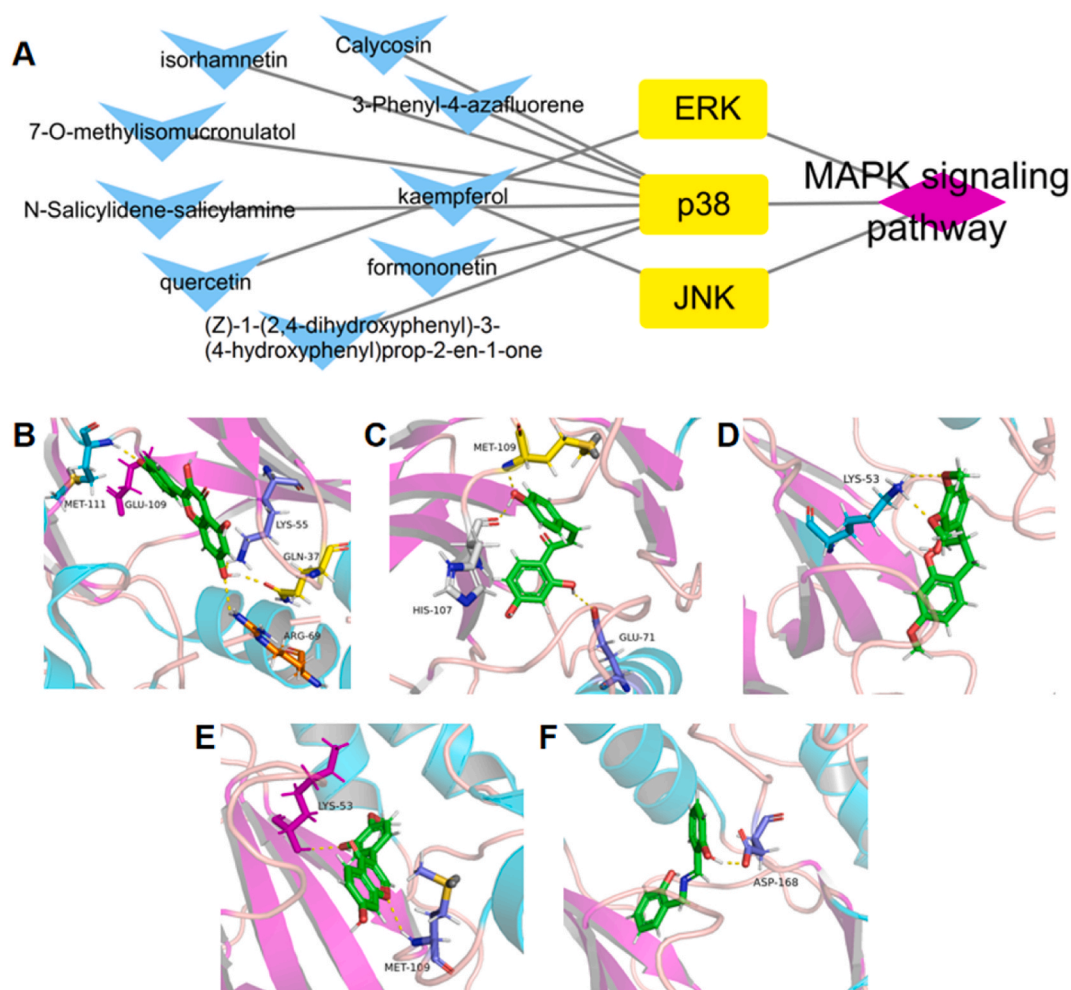


**Fig. 8.** Molecular docking. A: Network diagram of active ingredients and the key proteins in MAPK signaling pathway. Purple nodes represent MAPK signaling pathway, yellow nodes represent pathway proteins, and blue nodes represent potential active components. B: Binding mode of JNK (PDB ID: 3PZE) to kaempferol. C–F: Binding modes of p38 (PDB ID: 1WBW) to (z)-1-(2,4-dihydroxyphenyl)-3-(4-hydroxyphenyl)prop-2-en-1-one, 7-O-methylmalonulol, calycosin and N-salicylidene-salicylamine, respectively. (For interpretation of the references to color in this figure legend, the reader is referred to the Web version of this article.)

astragalus flavonoid that can rapidly and significantly activate the Ras-Raf-p38MAPK signaling pathway, resulting in an increase in the ratio of Bax/Bcl-2, which can lead to apoptosis. By RT-PCR and Western Blot assays, verisoflavone was shown to significantly upregulate ER $\beta$ , downregulate miR-375, and inhibit the growth of tumor cells [37,38]. N-salicylidene-salicylamine is derived from ginseng [39], which has pharmacological effects on multiple systems of the human body, especially the circulatory system, hematopoietic system, and central nervous system, and shows anti-tumor effects. Overall, our results suggest that the above ingredients may be the active ingredients of Aidi that are responsible for its effect against PCa; however, this needs further experimental verification.

In addition, this study also conducted a study on the composition of Aidi. The elucidation of chemical components is a key link in the modernization research of traditional Chinese medicine. Currently, liquid chromatography-mass spectrometry (LC-MS) has become the preferred method for fundamental research on traditional Chinese medicine. This experiment is based on the flexible scanning technology of quadrupole time-of-flight tandem mass spectrometer (Q-TOF/MS), and uses an ultra-high performance liquid chromatography analysis system to study the chemical composition of Aidi. Analysis results: Representative peak intensity chromatograms collected under positive and negative ion modes of Aidi include positive and negative ion modes, identifying 31 chemical components of Aidi. This includes 12 types of ginsenosides, including ginsenoside C, ginsenoside La, ginsenoside F1, ginsenoside F2, ginsenoside F4 (20E), ginsenoside Re, ginsenoside Rf, ginsenoside Rh1, ginsenoside Rh4, ginsenoside Rg6, ginsenoside Rg5, and ginsenoside Rg3. Ginsenoside is a steroid compound with various important pharmacological activities such as enhancing immunity and inhibiting tumors. The above suggests that ginsenosides may be a component of Aidi's action on tumors.

In conclusion, this study confirmed that: (1) Aidi can inhibit the growth and metastasis of PCa cells *in vitro*; (2) Aidi can induce DU145 cell apoptosis and G2/M phase cycle arrest; (3) Aidi can inhibit the proliferation of PCa cells by activating the p38 and JNK signaling pathways. (4) (Z)-1-(2,4-dihydroxyphenyl)-3-(4-hydroxyphenyl) prop-2-en-1-one, 7-O-methylsomalonulol, kaempferol,

Calycosin, and N-Salicylidene salicylamine may be the active components of Aidi that inhibit PCa.

However, this study only explored the action and molecular mechanism of Aidi in inhibiting the proliferation and metastasis of PCa cells *in vitro*, which is still lack of experimental verification *in vivo*. In the future research, we will use the tumor bearing mouse model to explore the anti-PCa effect of Aidi, so as to provide a reference for further application of Aidi in the clinical treatment of PCa. We have only verified the MAPK pathway predicted by network pharmacology at present. In the follow-up study, we will verify the predicted other related pathways to more comprehensively explain the mechanism of action of Aidi against PCa.

### Funding details

This work was supported by Guangxi Natural Science Foundation (2023JJB140141), Guangxi Science and Technology Project (FANGKE ZY20221502), and Advanced Innovation Teams and Xinghu Scholars Program of Guangxi Medical University.

### Disclosure statement

There are no financial conflicts of interest to disclose.

### Data availability statement

Data included in article/supp. material/referenced in article.

### CRedit authorship contribution statement

**Sheng Guo:** Writing – review & editing, Writing – original draft, Software, Resources, Project administration, Conceptualization. **Qiuping Zhang:** Writing – review & editing, Project administration, Funding acquisition. **Xiaolan Li:** Writing – review & editing, Validation, Software, Conceptualization. **Xiaoxiang Yu:** Conceptualization. **Taijin Lan:** Writing – original draft. **Weiquan Zhang:** Software. **Yaoyao Han:** Software. **Xin Chen:** Data curation. **Xin Yang:** Visualization, Investigation. **Hongwei Guo:** Writing – review & editing, Conceptualization.

### Declaration of competing interest

The authors declare the following financial interests/personal relationships which may be considered as potential competing interests: Hongwei Guo reports financial support was provided by Guangxi Science and Technology Project (FANGKE ZY20221502), and Advanced Innovation Teams and Xinghu Scholars Program of Guangxi Medical University. Xin Yang reports financial support was provided by Guangxi Natural Science Foundation (2023JJB140141). If there are other authors, they declare that they have no known competing financial interests or personal relationships that could have appeared to influence the work reported in this paper.

### Acknowledgments

Hongwei Guo contributed to designing the work. Sheng Guo and Xin Yang wrote the manuscript. Sheng Guo, Quipping Zhang and Xiaolan Li conducted the main experiments and analysis of the data. Xiaoxiang Yu, Taijin Lan, Weiquan Zhang, Yaoyao Han, Xin Chen provided technical assistance. Hongwei Guo and Xin Yang contributed reagents/materials/analysis tools. All authors read and approved the final version.

### Appendix A. Supplementary data

Supplementary data to this article can be found online at <https://doi.org/10.1016/j.heliyon.2024.e29720>.

### References

- [1] F. Bray, J. Ferlay, I. Soerjomataram, et al., Global Cancer Statistics 2018: GLOBOCAN estimates of incidence and mortality worldwide for 36 cancers in 185 countries, *CA A Cancer J. Clin.* 68 (6) (2018) 394–424.
- [2] G. Fuzhentao, S. Zhang, et al., Analysis of prostate cancer incidence and death in China in 2015, *Chin. J. Oncol.* 42 (9) (2020) 718–722.
- [3] X.Y. Gu, R.S. Zheng, S. Zhang, et al., Analysis on the incidence trend and age change of prostate cancer in China's tumor registration areas from 2000 to 2014, *Chin. J. Prev. Med.* 52 (6) (2018) 586–592.
- [4] L. Xu, J.M. Guo, Standard and latest progress in the treatment of advanced prostate cancer, *J. Pract. Oncol.* 35 (2) (2020) 100–106.
- [5] E.A. Benaim, C.M. Pace, C.G. Roehrbom, Gleason score predicts androgen independent progression after androgen deprivation therapy, *Eur. Urol.* 42 (1) (2002) 12–17.
- [6] X.Y. Wei, J.S. Peng, L. Huang, et al., Relationship between TMPRSS2-ERG fusion gene and survival rate of metastatic castration resistant prostate cancer after chemotherapy, *J Cap Med Univ.* 41 (1) (2020) 103–107.
- [7] Y. Zhu, Consensus of experts in diagnosis and treatment of castration resistant prostate cancer in China, *Chin. J. Surg.* 54 (7) (2016) 481–484.

- [8] T.Y. Li, Z.J. Chen, Y.S. Li, Research progress of androgen receptor therapy with traditional Chinese medicine, *Chinese J Trad Chinese Med.* 37 (6) (2019) 1331–1334.
- [9] J.J. Li, C.M. Zheng, H.L. Zhou, et al., Investigation and analysis of clinical application of Aidi injection, *Oncology* 6 (4) (2016) 313–317.
- [10] Taijin Lan, Li Qiaofeng, Chang Ming, et al., Lei-gong-gen formula granule attenuates hyperlipidemia in rats via cGMP-PKG signaling pathway, *J. Ethnopharmacol.* 260 (2020) 112989.
- [11] Xin Chen, Zhuo Luo, Xi Liu, et al., *Marsdenia tenacissima* (Roxb.) Moon injection exerts a potential anti-tumor effect in prostate cancer through inhibiting ErbB2-GSK3 $\beta$ -HIF1 $\alpha$  signaling axis, *J. Ethnopharmacol.* 295 (2022) 115381.
- [12] Li Xiaolan, He Song, Wei Liang, et al., *Marsdenia tenacissima* (Roxb.) Moon injection induces apoptosis of prostate cancer by regulating AKT/GSK3 $\beta$ /STAT3 signaling axis, *Chin. J. Nat. Med.* 20 (0) (2022) 1–15.
- [13] Chang Ming, Dan Zhu, Yanjiang Chen, et al., Total flavonoids of Litchi seed attenuate prostate cancer progression via inhibiting AKT/mTOR and NF-kB signaling pathways, *Front. Pharmacol.* 12 (2021) 758219.
- [14] Hongwei Guo, Hua Luo, Hebao Yuan, et al., Litchi seed extracts diminish prostate cancer progression via induction of apoptosis and attenuation of EMT through Akt/GSK-3 $\beta$  signaling, *Sci. Rep.* 7 (2017) 41656.
- [15] Li Qiaofeng, Lan Taijin, Songhua He, et al., A network pharmacology-based approach to explore the active ingredients and molecular mechanism of Lei-gong-gen formula granule on a spontaneously hypertensive rat model, *Chin. Med.* 16 (1) (2021) 99.
- [16] Wei Xue, Jie Hao, Qiuping Zhang, et al., Chlorogenic acid inhibits epithelial-mesenchymal transition and invasion of breast cancer by down-regulating LRP6, *J. Pharmacol. Exp. Therapeut.* 384 (2) (2023) 254–264.
- [17] J.M. Davies, R.M. Goldberg, Treatment of metastatic colorectal cancer, *Semin. Oncol.* 38 (4) (2011) 552–560.
- [18] G.P. Gupta, J. Massague, Cancer metastasis: building a framework, *Cell* 127 (4) (2006) 679–695.
- [19] S. Wang, Y. Li, C. Xing, et al., Tumor microenvironment in chemoresistance, metastasis and immunotherapy of pancreatic cancer, *Am. J. Cancer Res.* 10 (7) (2020) 1937–1953.
- [20] H. Mohamed, C. Haglund, L. Jouhi, et al., Expression and role of E-cadherin, beta-catenin, and vimentin in human papillomavirus-positive and human papillomavirus-negative oropharyngeal squamous cell carcinoma, *J. Histochem. Cytochem.* 68 (9) (2020) 595–606.
- [21] L.J. Zhang, Study on the Role of Akt1/2 in the Progression of Castration Resistant Prostate Cancer [dissertation], Xinxiang Medical College, 2019.
- [22] X.L. Zhang, Y.X. Ye, Z.H. Ye, Effect of mir-545-3p on proliferation and apoptosis of prostate cancer cells by inhibiting VEGFA/VEGFR2 signaling pathway, *Chinese J Sexual Sci* 29 (9) (2020) 5–10.
- [23] L. Zheng, H.L. Zheng, X.G. Liu, Housekeeper gene GAPDH should be considered carefully as an internal reference in tumor and aging tissues, *Chinese J Biochem Mol Biol* 34 (4) (2018) 385–389.
- [24] Y. Sun, W.Z. Liu, T. Liu, et al., Signaling pathway of MAPK/ERK in cell proliferation, differentiation, migration, senescence and apoptosis, *J. Recept. Signal Transduct. Res.* 35 (6) (2015) 600–604.
- [25] M. Martini, M.C. De Santis, L. Braccini, et al., PI3K/AKT signaling pathway and cancer: an updated review, *Ann. Med.* 46 (6) (2014) 372–383.
- [26] Y. Jiang, LPS mediated signal transduction in cell activation: a study on the pathway from CD14 to p38MAPK, *Adv Physiol Sci* 1999 (1) (1999) 31–36.
- [27] Z. Zuo, J. Liu, Z. Sun, et al., ERK and c-Myc signaling in host-derived tumor endothelial cells is essential for solid tumor growth, *P NATL ACAD SCI USA* 120 (1) (2022) e2211927120.
- [28] T.E. Hybel, D. Dietrichs, J. Sahana, et al., Simulated microgravity influences VEGF, MAPK, and PAM signaling in prostate cancer cells, *Int. J. Mol. Sci.* 21 (4) (2020) 1263.
- [29] S. Li, K.W. Fong, G. Gritsina, et al., Activation of MAPK Signaling by CXCR7 leads to enzalutamide resistance in prostate cancer, *Cancer Res.* 79 (10) (2019) 2580–2592.
- [30] B.Y. Shorning, M.S. Dass, M.J. Smalley, et al., The PI3K-AKT-mTOR pathway and prostate cancer: at the crossroads of AR, MAPK, and WNT signaling, *Int. J. Mol. Sci.* 21 (12) (2020) 4507.
- [31] W.Z. Wang, L. Li, M.Y. Liu, et al., Curcumin induces FasL-related apoptosis through p38 activation in human hepatocellular carcinoma Huh7 cells, *Life Sci.* 92 (6–7) (2013) 352–358.
- [32] S. Ghatan, S. Lamer, Y. Kinoshita, et al., p38 MAP kinase mediates bax translocation in nitric oxide-induced apoptosis in neurons, *J. Cell Biol.* 150 (2) (2000) 335–347.
- [33] Y Feng, H Cao, D Wang, et al., JNK promotes the progression of castration-resistant prostate cancer, *ACTA BIOCHIM* 70 (4) (2023) 817–822, <https://doi.org/10.18388/abp.2020.6610>.
- [34] V.G. Keshamouni, D.A. Arenberg, R.C. Reddy, et al., PPAR-gamma activation inhibits angiogenesis by blocking ELR+CXC chemokine production in non-small cell lung cancer, *Neoplasia* 7 (3) (2005) 294–301.
- [35] R. Li, T. Wheeler, H. Dai, et al., High level of androgen receptor is associated with aggressive clinicopathologic features and decreased biochemical recurrence-free survival in prostate: cancer patients treated with radical prostatectomy, *Am. J. Surg. Pathol.* 28 (7) (2004) 928–934.
- [36] X.Q. Lei, A. Chen, Y. Liu, et al., Research progress on pharmacological action of kaempferol, *Res Trace Elements Health* 34 (2) (2017) 61–62.
- [37] J. Chen, R. Hou, X. Zhang, et al., Calycosin suppresses breast cancer cell growth via ERbeta-dependent regulation of IGF-1R, p38 MAPK and PI3K/Akt pathways, *PLoS One* 9 (3) (2014) e91245.
- [38] D.Q. Zhang, H.B. Wang, S.F. Wang, et al., Research progress on bioactivity of pistil isoflavones, *Chinese J Trad Chinese Med* 40 (22) (2015) 4339–4345.
- [39] J.X. Zhang, Simulation Study on the Action Mechanism of Traditional Chinese Medicine Based on Chemical Informatics, Dalian University of Technology, 2015 [dissertation].